Possibility of a spin-Peierls state in $CuSiO_3$ from electronic structure theory

H. Rosner,* S.-L. Drechsler, K. Koepernik, R. Hayn, and H. Eschrig
Institut für Festkörper- und Werkstofforschung Dresden, P.O. Box 270116, D-01171 Dresden, Germany
(Received 12 April 2000; published 26 January 2001)

Electronic structure calculations are presented for the well-known $CuGeO_3$ and the recently discovered isostructural $CuSiO_3$ compounds. The magnitude of the dispersion in chain direction is considerably smaller for $CuSiO_3$, whereas the main interchain couplings are rather similar in both compounds. Starting from extended one-band, tight-binding models fitted to the band structures, the exchange integrals were estimated for both compounds in terms of a spatially anisotropic Heisenberg model. Remarkable, frustrating second-neighbor couplings are found both for intra- and interchain interactions. A magnetic moment of about $0.35\mu_B$ is predicted for $CuSiO_3$ in the Néel state.

DOI: 10.1103/PhysRevB.63.073104 PACS number(s): 71.15.Mb, 71.20.−b, 75.30.Et

Low-dimensional spin systems such as chains or ladders are of fundamental interest for contemporary solid-state physics due to their peculiar electronic and magnetic properties. During the last years, many related materials have been found within the cuprate family, famous for the high-temperature superconductivity. All cuprates contain CuO_4 plaquettes. In most cases, it is energetically favorable to connect these plaquettes by the formation of chains or planes. According to the number ($n=1,2$) of oxygen atoms shared by adjacent plaquettes, these compounds can be classified as so-called edge-shared ($n=2$) or corner-shared ($n=1$) compounds.

Obviously, the type of sharing affects strongly the physical properties of the compounds under consideration. For example, corner sharing leads to strong antiferromagnetic coupling between neighboring plaquettes compared with the weak interchain interactions.[1] As a result, the straight CuO_3 chain in Sr_2CuO_3 is the best known realization of the one-dimensional spin-1/2 Heisenberg model,[2] with an in-chain exchange coupling of about 2200 K, but with a Néel temperature of only 5 K and with an extremely small ordered magnetic moment of about $0.06\mu_B$,[3] both due to a small residual interchain exchange coupling. Spin-charge separation in the excitation spectra could be observed for Sr_2CuO_3 and for the double chain compound $SrCuO_2$.[4]

Somewhat surprisingly, in contrast to the similarity between different corner-shared chain compounds, the magnetic properties in the edge-shared chain family exhibit a remarkable variance. Thus, the edge-shared CuO_2 plaquettes in Li_2CuO_2 order antiferromagnetically with a ferromagnetic arrangement along those chains and with a large ordered moment of $0.9\mu_B$,[5] whereas the same chain in $CuGeO_3$ shows a spin-Peierls transition at low temperatures.[6] Antiferromagnetically ordered chains were observed in $Cu_{1-x}Zn_xGeO_3$ for small concentrations of Zn impurities.[7] It is noteworthy that, even for the intensively studied $CuGeO_3$, a consensus with respect to the quantitative description of competing or complementary interactions such as the interchain coupling, frustration, and spin-phonon coupling has not been reached so far,[8,9] despite the achieved qualitative understanding of their influence on different magnetically ordered states.

Naturally, the magnetic properties depend very sensitively on the electronic interactions in these systems. Therefore, a comparative study of the electronic properties of closely related systems can shed light on the interactions responsible for the magnetically ordered states mentioned above. In this context, the recent discovery and first investigations of the long searched-for compound $CuSiO_3$,[10] which is isostructural to the prototypical inorganic spin-Peierls system $CuGeO_3$ is of great scientific interest. The crystal structure of $CuSiO_3$ is shown in Fig. 1. The most important feature for the magnetic properties are the planar edge-shared CuO_2 chains running along the **c** direction. These chains are very similar to those of $CuGeO_3$. The Cu-O(2) bond length in $CuSiO_3$ ($CuGeO_3$) is 1.941 Å (1.942 Å), the Cu-O(2)-Cu bonding angle is 94° (99°).

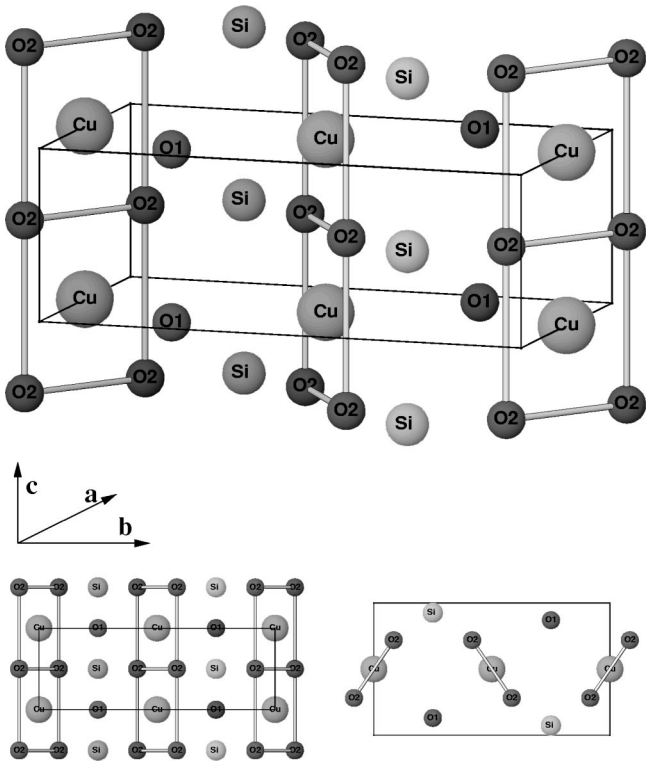

FIG. 1. The orthorhombic unit cell of the $CuSiO_3$ crystal, perspective view (top), front view (down left) and top view (down right). The edge-shared cuprate chains run along the **c** direction and are canted against each other.

Thus, the question arises whether the very recently observed phase transition[11] near 8 K does point to a new inorganic spin-Peierls system or to another ordered state realized at low temperature. To get theoretical insight into possible scenarios, we present here comparative band-structure calculations and tight-binding examinations for $CuSiO_3$ and $CuGeO_3$. In this context we note that for the latter compound several band-structure calculations have been reported,[12–14] but to our knowledge the interchain interaction has not been analyzed in detail.

The relevant electronic structure of these materials is very sensitive to details of hybridization and charge balance. In order to obtain a realistic and reliable hopping part of a tight-binding Hamiltonian, band-structure calculations were performed using the full-potential nonorthogonal local-orbital minimum-basis scheme[15] within the local density approximation (LDA). In the scalar relativistic calculations we used the exchange and correlation potential of Perdew and Zunger.[16] Cu($4s$,$4p$,$3d$), O($2s$,$2p$,$3d$), Ge($3d$,$4s$,$4p$,$4d$), and Si($2p$,$3s$,$3p$,$3d$) states, respectively, were chosen as minimum basis set. All lower-lying states were treated as core states. The inclusion of Ge $3d$ and Si $2p$ states in the valence states was necessary to account for non-negligible core-core overlaps. The O and Si $3d$, as well as the Ge $4d$ states were taken into account to increase the completeness of the basis set. The spatial extension of the basis orbitals, controlled by a confining potential[17] $(r/r_0)^4$, was optimized to minimize the total energy.

The results of the paramagnetic calculation[18] for $CuSiO_3$ [see Fig. 2(a)] and $CuGeO_3$ [see Fig. 2(b); we find similar results as in Refs. 12–14] show a valence-band complex of about 10 eV width with two bands crossing the Fermi level in both cases. These two bands are well separated from the rest of the valence-band complex and show mainly Cu $3d$ and O(2) $2p$ character in the analysis of the corresponding partial densities of states (not shown). We note that the occupancy of the two O(2) $2p$ orbitals along and perpendicular to the chain (lying in the plaquette planes) is rather different, but it is almost identical for the corresponding orbitals in both compounds. Therein, we found only a small admixture of O(1) $2p$ and Ge $4s$ and $4p$ states, respectively, with a total amount of few percent. The examination of the eigenstates of the latter bands at high-symmetry points yields an antibonding character typical for cuprates. Here, these relatively narrow antibonding bands are half filled. Therefore, strong correlation effects can be expected that explain the experimentally observed insulating ground state. Despite almost perfect qualitative one-to-one correspondence of all valence bands and main-peak structures in the densities of states (compare right panels in Fig. 2), the most important differences between both compounds occur for the antibonding bands [shown in detail in Fig. 2(c)]. Therefore, we restrict ourselves to the extended tight-binding analysis and the discussion of these antibonding bands.

The dispersion of these bands has been analyzed in terms of nearest-neighbor transfer (NN), next-nearest-neighbor transfer (NNN) and higher-neighbor terms in chain direction, but only NN hopping and a diagonal transition term between

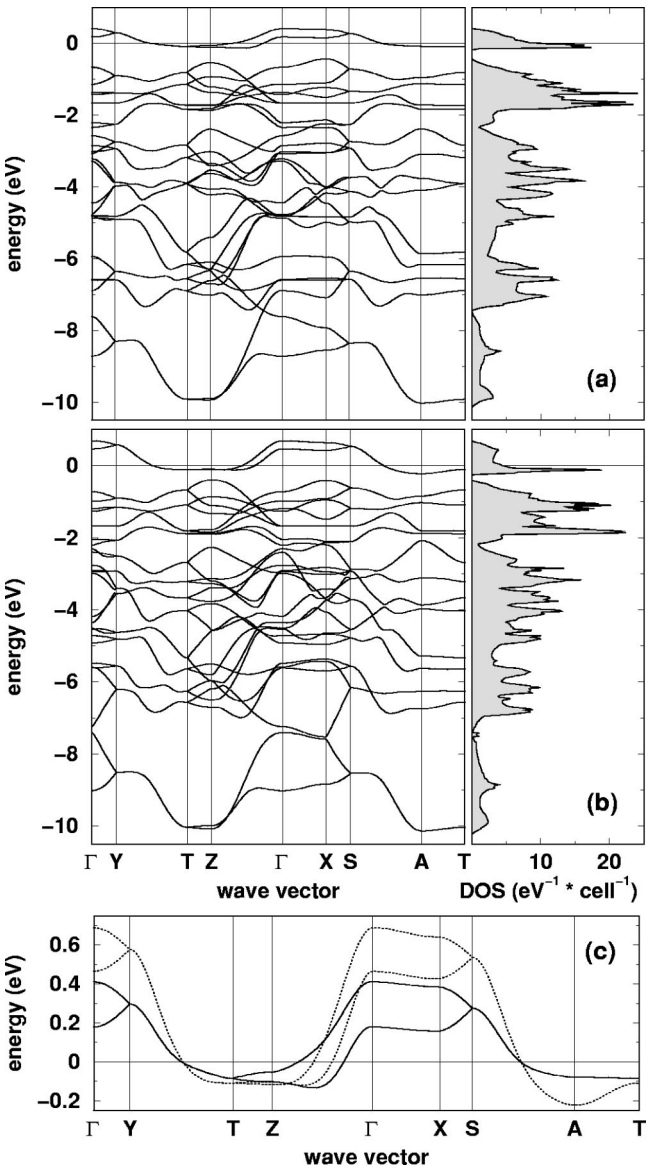

FIG. 2. Band structure and total density of states for $CuSiO_3$ (a), $CuGeO_3$ (b), and the zoomed antibonding bands (c) ($CuSiO_3$ full lines, $CuGeO_3$ dashed lines). The Fermi level is at zero energy. The notation of the symmetry points is as follows: $Y=(010)$, $T=(011)$, $Z=(001)$, $X=(100)$, $S=(110)$, and $A=(111)$. The chain direction corresponds to Y-T, Z-Γ and S-A.

the CuO_2-chains have been considered (see Fig. 3). Then, the corresponding dispersion relation takes the form

$$E(\vec{k}) = -2\Big(\sum_{m=1,4} t_{mz}\cos(mz) + \cos(x)[t_x + 2t_{xz}\cos(z)] + \cos(y/2)[t_y + 2t_{yz}\cos(z) + 2t_{xy}\cos(x)] \Big), \qquad (1)$$

where $x=k_x a$, $y=k_y b$, $z=k_z c$. Notice that in our effective one-band description the upper band [see Fig. 2(c)] e.g., along Γ–X corresponds to $k_y=0$, whereas the lower one corresponds to $k_y=2\pi/b$. The assignment of the parameters has been achieved by two numerically independent proce-

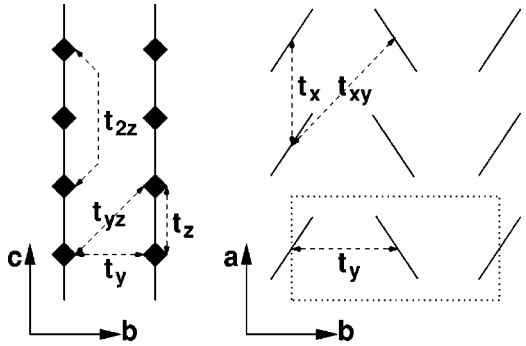

FIG. 3. Schematical chain and stack arrangement of CuO_2 plaquettes, respectively, and considered transfer processes within the bc plane (left panel) and in the ab plane (right panel).

dures: By straightforward, least-squares fitting of the whole antibonding band in all directions and by using the bandwidths, the slopes, and the curvatures at special selected high-symmetry points. The latter procedure has the advantage to be less affected by hybridization effects from lower-lying bands near the bottom of the antibonding band (being of some relevance near the Z point in Fig. 2).

The results are shown in Table I. The errors can be estimated between 1% for the large and 10% for the small parameters from the difference of both mentioned above fitting procedures. The analyzed antibonding bands of both compounds exhibit a rather similar shape except near the Z points, where the effect of hybridization with lower-lying bands is visible [see Fig. 2(c)]. Recall that the main difference to the corner-shared chains as e.g., in Sr_2CuO_3, is a much smaller in-chain NN transfer due to the different geometry.

In spite of the qualitative similarity, the calculated values for the transfer integrals are quite different. The in-chain dispersion is nearly twice as large for $CuGeO_3$ in comparison to $CuSiO_3$. This can be attributed mainly to the larger Cu-O-Cu bond angle in $CuGeO_3$ (99° and 94°, respectively). However, this geometrical effect is somewhat reduced by the different on-site energies of the oxygen orbitals along and perpendicular to the chain (lying in the plaquettes planes). The latter difference is reflected by the larger separation of the corresponding bands at the Z point in $CuSiO_3$ (see Fig. 2).

The interchain dispersions in b direction are comparable. For both compounds, we find also rather significant diagonal hopping terms t_{yz} that are reflected by different dispersions along the X-S and the T-Z directions. Somewhat surprisingly, we found a sizeable dispersion in x direction for $CuGeO_3$ but only a very weak one for the $CuSiO_3$ counterpart.

TABLE I. Transfer integrals t_i (in meV) of the extended one-band tight-binding model for $CuGeO_3$ and $CuSiO_3$. The remaining omitted terms from Eq. (1) were found to be irrelevant.

	t_z	t_{2z}	t_{3z}	t_x	t_y	t_{yz}
$CuGeO_3$	−175	−51	−5.5	−20	−34.1	−20.6
$CuSiO_3$	−88	−31	−4.5	−2.4	−36	−21.2

TABLE II. Exchange parameters J_i (in meV) for $CuGeO_3$ and $CuSiO_3$, and local magnetic moments (in μ_B) in the Néel state derived from them (see text). The experimental value μ_{ex} is an average over various studies mentioned in the text.

	J_1^{AF}	J_1	J_2	J_x	J_y	J_{yz}	μ_{th}	μ_{exp}
$CuGeO_3$	29	15	2.5	0.4	1.11	0.4	0.17	0.21
$CuSiO_3$	7.4	3.8	0.9	0.006	1.25	0.43	0.35	unknown

From the transfer integrals discussed above, we conclude that both compounds are not so well-defined quasi-one-dimensional systems as compared to the corner-shared CuO_3 chain compounds.[1,19] The interchain coupling is rather significant for $CuGeO_3$, and $CuSiO_3$ can even be regarded as an anisotropic two-dimensional system. Since increasing interchain coupling tends to destabilize the spin-Peierls state,[20] a Néel ordered antiferromagnetic ground state might be expected for $CuSiO_3$ in contrast to the spin-Peierls state realized in $CuGeO_3$.

The obtained transfer integrals enable us to estimate the relevant exchange integrals J. This knowledge is crucial for the derivation and examination of magnetic model Hamiltonians of the spin-1/2 Heisenberg type frequently used in the literature:

$$H_{spin}=\sum_{ij}{}' J_{ij}\vec{S}_i\vec{S}_j . \tag{2}$$

In general, the total exchange J can be divided into an antiferromagnetic and a ferromagnetic contribution $J=J^{AF}+J^{FM}$. In the strongly correlated limit, valid for typical cuprates, the former can be calculated in terms of the one-band extended Hubbard model $J_{ij}^{AF}=4t_{ij}^2/(U-V_{ij})$. The indices i and j correspond to nearest and next-nearest neighbors, U is the on-site Coulomb repulsion and V_{ij} is the intersite Coulomb interaction. From experimental data[21] mapped from the standard pd model onto the one-band description, one estimates $U-V\sim 4.2$ eV. For the sake of simplicity, we neglect the difference in the quantity U-V in the compounds. The calculated values for the exchange integrals are given in Table II.

The value of the NN exchange integral $J_1^{AF}\sim 30$ meV in $CuGeO_3$ exceeds the experimental values of about 11 meV from inelastic neutron-scattering data,[22] about 14 meV from magnetic susceptibility,[23] and about 22 meV from Raman scattering.[24] This points to a significant ferromagnetic contribution due to the Goodenough-Kanamori-Anderson–type interaction.[25] In the following, we shall adopt 15 meV for the resulting total exchange coupling J_1 as a representative value, suggested by the average of the above-mentioned experimental data. Owing to the lack of experimental data we assume the same ratio J_1/J_1^{AF} in $CuSiO_3$ as in $CuGeO_3$, suggested by the quite similar O(2) $2p$ orbital occupancies mentioned above. For the latter compound, we note the reasonable agreement with the available experimental data and

most of our calculated antiferromagnetic values for the remaining exchange parameters. Hence, further possible ferromagnetic contributions seem to be less relevant and are neglected in the following considerations.

Further simplification can be obtained mapping J_1 and the frustrated NN term J_2 onto an effective intrachain coupling $J_\parallel = J_1 - 1.12J_2$.[26] The calculated values for $J_\parallel$ are 12.2 meV for $CuGeO_3$ and 2.8 meV for $CuSiO_3$, respectively. The latter value is close to the value of 2 meV reported by Baenitz *et al.* from a one-dimensional fit of magnetic susceptibility data.[11] We find also a considerable interchain frustration $J_{yz} = \beta J_y$ with $\beta = 0.36$ (0.34) for the Ge- (Si-) compound. This is in good agreement with the suggestions of Uhrig[8] $\beta \approx 0.5$ for $CuGeO_3$.

Transferring the above-mentioned idea to map frustrating terms onto one effective coupling,[26] we adopt $J_\perp = J_y - 2J_{yz}$ for the effective interchain exchange parameters in b direction. The factor of 2 is introduced to account for approximately the twice as large number of second neighbors. The effective anisotropy ratio $R = J_\perp / J_\parallel$ measures approximately the magnitude of quantum fluctuations. In the crossover region between one and two dimensions, quantum fluctuations do strongly affect the magnitude of the staggered magnetization m and the local Cu moment $\mu = g_L n_d m$ at $T = 0$ for a Néel ground state, where $g_L = 2.06$ to 2.26 (Ref. 27) denotes the (anisotropic) Landé-factor (tensor) for Cu^{2+} in $CuGeO_3$ and $n_d \approx 0.8$ is the hole occupation number of the related Cu $3d$ plaquette orbital. Using the expression

$$m = 0.39\sqrt{R}(1 + 0.095R)\ln^{1/3}(1.3/R), \qquad (3)$$

taken from Ref. 28, we arrive at $0.17\mu_B$ in reasonable agreement[29] with the neutron data 0.22 ± 0.02 (Ref. 30) and 0.2 (Ref. 31) for the disorder-induced Néel state achieved below 4.5 K in Zn-doped $CuGeO_3$. The same approach predicts a significantly larger value of about $0.35\mu_B$ for $CuSiO_3$ realized in a possible Néel state.

To summarize, our LDA-FPLO calculation reveals valuable insight into the relevant couplings of $CuGeO_3$ and $CuSiO_3$. We can classify $CuGeO_3$ as a quasi-one-dimensional compound with significant interchain interaction, whereas $CuSiO_3$ is closer to an anisotropic two-dimensional compound. The significantly reduced energy scale of the in-chain exchange interactions and the large interchain interaction in $CuSiO_3$ are less favorable for a spin-Peierls state than for a Néel order. However, due to the large frustrations, other states such as a spin-Peierls state cannot be excluded. Further investigations are required to elucidate the unknown ground state.

Note added in proof. Using the Lieb-Wu solution of the single-band 1D Hubbard model in the strong coupling limit, the effective repulsion U_{eff} can be estimated as $U_{eff} = E_g - 4t_1$. With the optical data of M. Bassi *et al.* [Phys. Rev. B **54**, R11030 (1996)] for $GeCuO_3$ $E_g = 3.46$ eV and our $t_1 = 0.175$ eV, one arrives at 4.14 eV just very close to the value of 4.2 eV stated above.

We acknowledge fruitful discussions with M. Baenitz, C. Geibel, W. Pickett, and G. Uhrig. This work was supported by individual grants of the DAAD (H.R.) and the DFG (H.E.).

*Present address: Department of Physics, University of California Davis, CA, 95616.

[1] H. Rosner *et al.*, Phys. Rev. B **56**, 3402 (1997).
[2] A. Tsvelik, *Quantum Field Theorie in Condensed Matter* (Cambridge University Press, Cambridge, 1995).
[3] K. M. Kojima *et al.*, Phys. Rev. Lett. **78**, 1787 (1997).
[4] C. Kim *et al.*, Phys. Rev. Lett. **77**, 4054 (1996).
[5] F. Sapiña *et al.*, Solid State Commun. **74**, 779 (1990).
[6] M. Hase *et al.*, Phys. Rev. Lett. **70**, 3651 (1993).
[7] M. Hase *et al.*, Phys. Rev. Lett. **71**, 4059 (1993).
[8] G. Uhrig, Phys. Rev. Lett. **79**, 163 (1997). In a recent work by C. Knetter and Ct. Uhrig [Phys. Rev. B (to be published)], $\beta = 0.22$ has been refined.
[9] G. Bouzerar *et al.*, Phys. Rev. B **60**, 15 278 (1999).
[10] H. H. Otto *et al.*, Z. Kristallogr. **214**, 558 (1999).
[11] M. Baenitz, Phys. Rev. B **62**, 12 201 (2000).
[12] L. F. Mattheiss, Phys. Rev. B **49**, 14 050 (1994).
[13] Z. S. Popovic *et al.*, J. Phys.: Condens. Matter **7**, 4594 (1995).
[14] Z. V. Sljivancanin *et al.*, Phys. Rev. B **56**, 4432 (1997).
[15] K. Koepernik *et al.*, Phys. Rev. B **59**, 1743 (1999).
[16] J. P. Perdew and A. Zunger, Phys. Rev. B **23**, 5048 (1981).
[17] H. Eschrig, *Optimized LCAO Method and the Electronic Structure of Extended Systems* (Springer, Berlin, 1989).
[18] For the tight-binding analysis, the paramagnetic solutions are sufficient. Magnetic local spin-density approximation (LSDA) solutions at lower energies were also found for both compounds showing insulating behavior, but due to the insufficient treatment of correlation in the LSDA, the calculated gaps are much too small.
[19] H. Rosner *et al.*, Physica B **259-261**, 1001 (1999).
[20] S. Inagaki *et al.*, J. Phys. Soc. Jpn. **52**, 3620 (1983).
[21] F. Parmigiani *et al.*, Phys. Rev. B **55**, 1459 (1997).
[22] L. P. Regnault *et al.*, Phys. Rev. B **53**, 5579 (1996).
[23] K. Fabricius *et al.*, Phys. Rev. B **57**, 1102 (1998).
[24] H. Kuroe *et al.*, Phys. Rev. B **55**, 409 (1997).
[25] P. W. Anderson, Phys. Rev. **115**, 2 (1959).
[26] A. Fledderjohann *et al.*, Europhys. Lett. **37**, 189 (1997).
[27] M. Honda *et al.*, J. Phys. Soc. Jpn. **65**, 691 (1996).
[28] A. W. Sandvik, Phys. Rev. Lett. **83**, 3069 (1999).
[29] The estimated moment should be regarded as a lower bound due to the neglected weak interaction in x direction that reduces further the quantum fluctuations. Due to the Mermin-Wagner theorem, this interaction is crucial for the finite Néel temperature not considered here.
[30] M. Hase *et al.*, J. Phys. Soc. Jpn. **65**, 273 (1996).
[31] Y. Sasago *et al.*, Phys. Rev. B **54**, 6835 (1996).